The impact of remote temperature anomalies on the strength and position of the Gulf Stream and on coastal sea level variability: a model sensitivity study

Tal Ezer[1] · Sönke Dangendorf[2]

Abstract

A regional numerical ocean model of the Gulf Stream (GS) and the US East Coast was used to conduct sensitivity experiments of the dynamic response to temperature anomalies originated at different Atlantic locations. In a series of experiments, temperature anomalies were injected into the model domain through inflow boundary conditions at either the Florida Current (FC), the Slope Current (SC), or the Sargasso Sea (SS), while holding all other inflows/outflows unchanged. The strong currents and meso-scale variability of the GS system result in fast transport of anomalies throughout the model domain and immediate response within days. During a period of 60 days, remote temperature anomalies of ± 2 °C induced about 5–12 cm change in coastal sea level, about 0.5–1.0 ms^{-1} change in velocity, and about 30–50 km shift in the GS position, and a significant increase in kinetic energy of the whole GS system. Warm anomaly entering into the GS from the south through the FC had the strongest impact, strengthening the GS and temporally lowering coastal sea level by as much as ~10 cm, compared with coastal sea level drop of ~2–3 cm when the same warm anomaly was coming from the SS. Cold or warm anomalies coming from the north through the SC caused a large shift in the GS path, which moved onshore in the Mid-Atlantic Bight (MAB) and offshore in the South Atlantic Bight (SAB). Observations taken in 2017 when 3 hurricanes disrupted the GS flow show similar links between temperature anomalies, the GS, and coastal sea level, as in the idealized model simulations. The results demonstrated how temperature anomalies due to storms or uneven climate warming can cause variations on the coast and increased kinetic energy near western boundary currents. Since coastal sea level is positively correlated with temperature, but negatively correlated with the strength of the GS, the non-linear combination of the two factors can result in unexpected spatiotemporal variability in coastal sea level. The study provides better understanding of how remote signals affect the coast.

Keywords Coastal sea level · Gulf Stream · Florida Current · Climate change

1 Introduction

One of the least understood and least predictable aspects of coastal sea level variability and sea level rise is the potential remote influence from open ocean signals. Examples of such signals include offshore storms that disrupt strong ocean currents like the Gulf Stream (Ezer et al. 2017; Ezer

✉ Tal Ezer
tezer@odu.edu

1 Center for Coastal Physical Oceanography, Old Dominion University, 4111 Monarch Way, Norfolk, VA 23508, USA

2 Department of River-Coastal Science and Engineering, Tulane University, New Orleans, LA, USA

2018, 2019b, 2020; Kourafalou et al. 2016; Todd et al. 2018) or the Loop Current (Oey et al. 2007); such storms can create temperature anomalies of at least 2–3 °C along the storm's path. Climatic changes in the Atlantic Warm Pool can create temperature anomalies of ~1 °C in the Florida Current (Domingues et al. 2018), and in recent decades, there are periods when western boundary currents can be as much as ~3–5 °C warmer than the mean SST of past decades, suggesting that these anomalies are connected to shifts in the jet stream and shifts in western boundary currents (Kohyama et al. 2021). The role of shifting western boundary currents due to climate change and variability is further emphasized in another recent study (Diabaté et al. 2021). Other remote influences on the coast include shifts in winds or air pressure (Woodworth et al. 2014; Piecuch et al. 2016), basin-scale baroclinic Rossby

waves (Hong et al. 2000; Calafat et al. 2018), or changes in the Atlantic Meridional Overturning Circulation (AMOC), in the Gulf Stream (GS) transport, or in the North Atlantic Oscillation (NAO) (Ezer et al. 2013; Ezer 2015, 2016; Woodworth et al. 2014, 2016; Little et al. 2019). While different mechanisms may dominate different regions, large-scale ocean dynamics control on coastal sea level can be found globally (Dangendorf et al. 2021). The different atmospheric and oceanic processes mentioned above can impact the coastal sea level in two main ways. First, changes in ocean densities due to spatial variations in temperature and salinity can impact steric sea level. Second, flows of major ocean currents are proportional to sea level gradients across the currents through the geostrophic balance, thus for example, the GS flow intensity was found in many studies to be anticorrelated with coastal sea level on the US East Coast on time scales ranging from days to decades (Ezer et al. 2013; Ezer 2015, 2016; Goddard et al. 2015; Park and Sweet 2015; Wdowinski et al. 2016). For the same reason, a shift in the position of the GS can also affect coastal sea level (e.g., see Fig. 2 in Ezer et al. 2013).

Note that the idea that variations in the GS can induce variations in sea level along the US East Coast is not new and had been suggested long time ago by observations (Blaha 1984) and models (Ezer 2001), but this connection received more attention in recent years since rising sea levels and increased coastal flooding became concerning issues (Ezer and Atkinson 2014), with debates whether "hotspots" of sea level rise may be linked with slowing down of the GS (Ezer et al. 2013; Sallenger et al. 2012; Valle-Levinson et al. 2017; Domingues et al. 2018). Better understanding of sea level variations due to remote influences will help predict future sea level rise and variability. Remote influences on coastal sea level in the western North Atlantic is especially complicated as they involve basin-scale atmospheric and oceanic phenomena such as NAO and AMOC, but also local meso-scale influences from eddies and the GS meanders. For example, a few days disruption in surface temperatures due to the passage of a hurricane will quickly spread throughout the GS system and may cause a long-term effect on the ocean and the coast that can last for many weeks after the storm disappeared (Ezer 2020). A period with unusually low NAO or weak AMOC can induce anomalous sea level rise and unexpected year-long unusual coastal flooding, as was the case for example in 2009–2010 (Ezer, 2015; Goddard et al. 2015).

Another aspect that links climate changes and ocean dynamics involves potential long-term changes in western boundary currents (WBCs). Recent studies, using sea surface temperature data, atmospheric reanalysis data, and climate models, suggest, for example, that some WBCs are intensifying and potentially shifting their path northward (Wu et al. 2012; Yang et al. 2016; Ezer and Dangendorf 2021). Though

the exact causes of these changes are not completely clear, one potential mechanism is a poleward shift and intensification in zonal winds. However, the recent study of Ezer and Dangendorf (2021) shows that wind kinetic energy and oceanic kinetic energy over WBC regions are only weakly linked, and instead the study suggested that increased oceanic kinetic energy is partly driven by uneven warming that increased spatial gradients of surface temperatures, sea level, and currents.
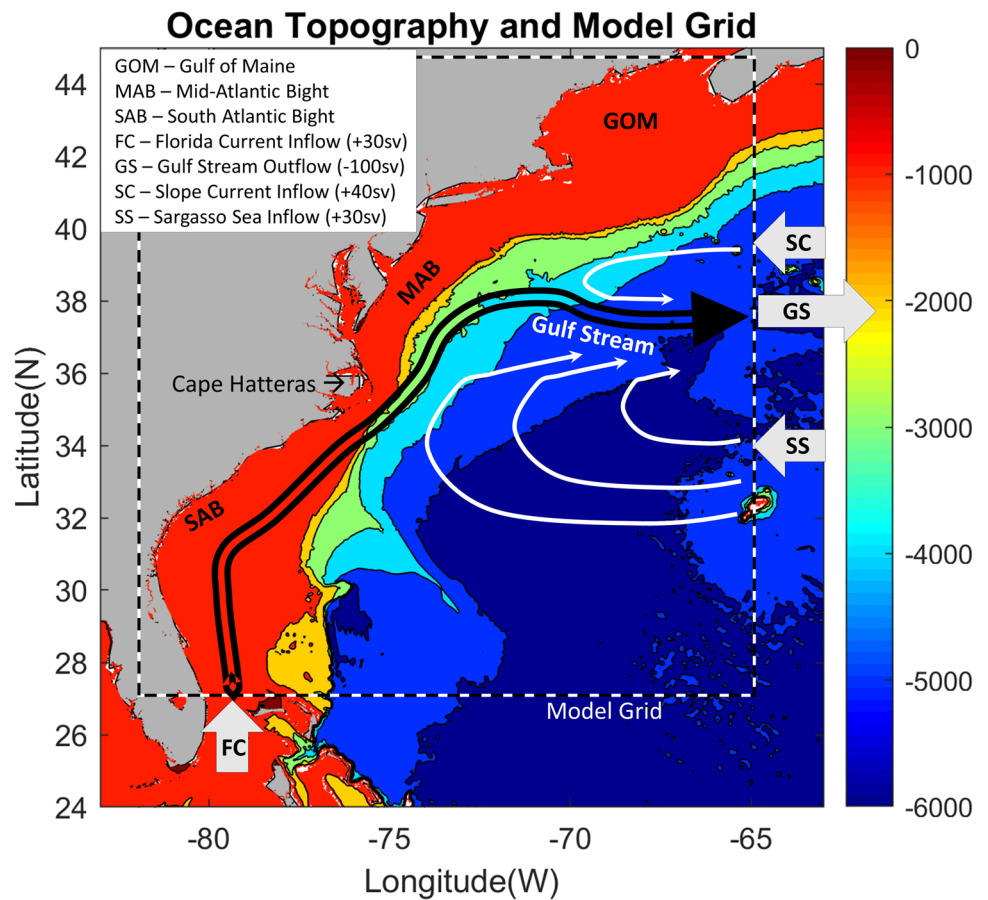
Since formation periods of temperature anomalies are irregular and they are formed by different forcing at different locations, it is difficult to study their impact on the coast using observations. Therefore, here sensitivity experiments using a regional numerical ocean model are conducted by introducing anomalous temperatures at different locations around the GS system and examining the response relative to a control experiment with fixed surface and lateral boundary conditions. These idealized experiments are not meant to be completely realistic—they can be viewed as process-oriented experiments to help isolate different mechanisms and examine whether spatial temperature variations in the open ocean can significantly impact the GS and the coast. Nevertheless, at the end of this study, some observations are shown to demonstrate that the idealized model results are qualitatively reasonable and helpful in better understanding of the processes involved.

The study is organized as follows. First, the model setting is described in Section 2, and then results of the different experiments are presented in Section 3, and finally a summery and conclusions are offered in Section 4.

2 Model description and experiments

The configuration of the regional numerical ocean model (Fig. 1) is the same as in several recent studies (Ezer 2016, 2018, 2019b), using a numerical ocean model code with generalized coordinates (Mellor et al. 2002; Ezer and Mellor 2004; a code evolved from the Princeton Ocean Model, POM) and a Mellor-Yamada turbulence scheme to provide vertical mixing. The model topography is based on the ETOPO5 data with minimum depth of 10 m. The Cartesian horizontal grid has 1/12° resolution (~6–8 km grid size), and the vertical terrain-following grid has 21 layers with higher resolution near the surface. The initial condition for all the experiments starts after 3 months spin up from monthly mean temperature and salinity data and a mean wind field that remains constant in time throughout all the simulations (so wind is not a factor when comparing different experiments). Surface heat fluxes are set to zero; since for the short simulations conducted here, air-sea interaction should not play a major role; this assumption is supported by studies that show that near western boundary currents, the role of advection is stronger than

Fig. 1 Bottom topography (color in meter) of the region and model domain (dashed line). The location of imposed model's inflows (Florida Current, FC; Slope Current, SC and Sargasso Sea, SS) and outflow (Gulf Stream, GS) are indicated by wide gray arrows; schematic of the GS flow (black arrow) and recirculation gyres (white arrows) are also shown

Ocean Topography and Model Grid

GOM – Gulf of Maine
MAB – Mid-Atlantic Bight
SAB – South Atlantic Bight
FC – Florida Current Inflow (+30sv)
GS – Gulf Stream Outflow (-100sv)
SC – Slope Current Inflow (+40sv)
SS – Sargasso Sea Inflow (+30sv)

surface heat flux by an order of magnitude (Kohyama et al. 2021). All simulations last for 60 days after the end of the spin up; the main purpose of the simulations is to examine the short-term dynamic response of the system to remote temperature anomalies coming from outside the model domain. Because of the strong currents and mesoscale activities of the region within this period, anomalies could propagate from the boundaries throughout the study area, as seen in the model (Ezer 2018, 2019b) and in observations (Ezer 2020). Open boundary conditions for velocities (Fig. 1) are fixed with 3 inflows and one outflow (transports R in Sverdrup; $1sv = 10^6$ m^{3}s^{-1}), and initial surface temperature (T):

1. The Florida Current (FC): (27° N, 79° W–80° W), inflow R = 30sv, T = 26.5–27 °C
2. The Slope Current (SC): (39.5° N–41° N, 65° W), inflow R = 40sv, T = 15.5–18 °C
3. The Sargasso Sea flow (SS): (35.5° N–36.9° N, 65° W), inflow R = 30sv, T = 21.5–22 °C
4. The Gulf Stream outflow (GS): (37° N–39.3° N, 65° W), outflow R = −100sv, T = 18–21 °C

The barotropic fixed flow is imposed as noted above, while the baroclinic flow is dynamically adjusted in a 1-degree buffer zone where temperature and salinity are relaxed toward observations. For more details on the model, see the studies mentioned above. During 60-day simulations, inflows and outflows are kept fixed, but temperature of one inflow at a time was changed keeping all other parameters unchanged. In each case, the temperature of one of the inflows was ramped up (warming case) or down (cooling case) over 8 days period up to 2 °C anomaly and then remained constant at the anomaly value for the remaining 52 days. This magnitude and time scale of change may be roughly similar, for example, to temperature changes due to the passage of an offshore hurricane (Ezer et al. 2017; Ezer 2018, 2020). The seven experiments conducted are as follows:

1. Control case—the only forcing is fixed imposed boundary transport (Fig. 1) and constant wind, so any time dependent variations are internal meso-scale variability of the GS system. The impact of different boundary conditions in the other experiments is evaluated by calculating the difference relative to the control case.

Fig. 2 Examples of the sea surface temperature (SST) during 60-day simulation of the control experiment (left panels), the +2 °C warming of the FC experiment (middle panels), and the anomaly difference between the two cases (right panels)
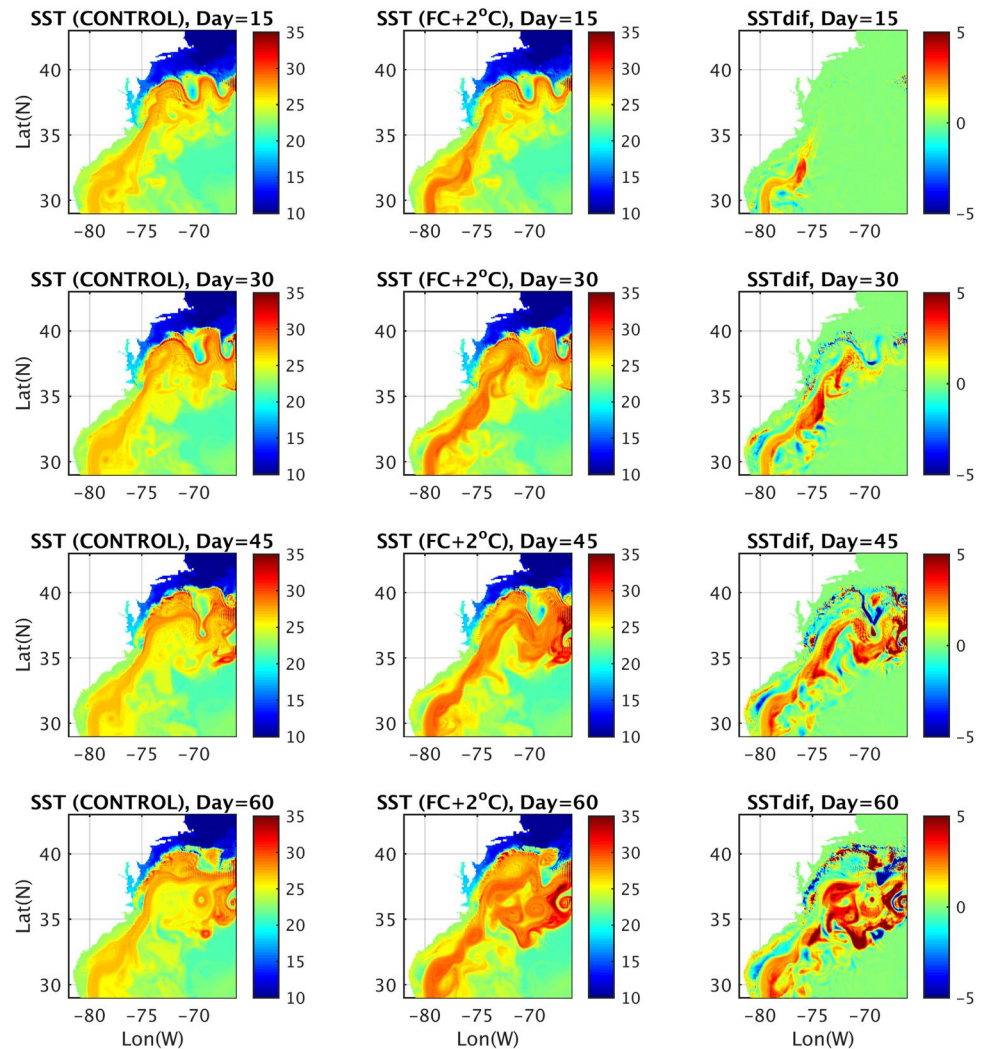
2. Florida Current warming case (FC + 2)—temperature of FC inflow is increased by 2 °C
3. Florida Current cooling case (FC-2)—temperature of FC inflow is decreased by 2 °C
4. Slope Current warming case (SC + 2)—temperature of SC inflow is increased by 2 °C
5. Slope Current cooling case (SC-2)—temperature of SC inflow is decreased by 2 °C
6. Sargasso Sea warming case (SS + 2)—temperature of SS inflow is increased by 2 °C
7. Sargasso Sea cooling case (SS-2)—temperature of SS inflow is decreased by 2 °C

Experiments 2/3, 4/5, and 6/7 will examine the impact of temperature anomalies coming from the south, the north, and the east, respectively, whereas either the GS itself

(cases 2/3) or the recirculation gyres (cases 4/5 and 6/7) are directly affected.

3 Results

3.1 The impact of temperature anomalies on coastal sea level

Examples of the sea surface temperature over 60 days in cases 1 (control) and 2 (FC + 2) are shown in Fig. 2, and they demonstrate the complex nature of the GS system. The temperature anomaly enters from the FC in the south propagates by the GS northeastward downstream and reached the eastern boundary of the model within ~ 30 days; by day 60, positive and negative

anomalies spread by meso-scale features (GS meanders and eddies) throughout the model domain (right panels of Fig. 2). Note that while the warm anomaly initially remains mostly offshore near the core of the GS, it can affect the coast later on and especially where the GS is close to the coast such as near Cape Hatteras, as shown later. A similar complex irregular anomaly field after 60 days is seen in other simulations (not shown) as well, so that the chaotic features of all experiments after 60 days do not tell us much without further quantitative analysis, as done below. The difference between the two simulations is partly due to the random and unpredictable nature of meso-scale variability, but comparisons (later) with the other simulations will help to see if there is an emerging pattern that may have resulted directly from the impact of the location of the anomaly and related ocean dynamics.

The impact of warm and cold FC anomalies on the coast is seen in the Hovmöller plot of coastal sea level anomaly as a function of time and latitude along the coast (Fig. 3a for FC + 2 and Fig. 3b for FC-2). One

clear result is the smaller response in the MAB (north of Cape Hatteras; latitude > 35.5° N) compared with changes of up to ~ 10 cm in the SAB. This result is consistent with several studies that showed different coastal response to forcing between the MAB and the SAB (Ezer 2016, 2019a; Woodworth et al. 2016; Valle-Levinson et al. 2017; Domingues et al. 2018). The different response between the two regions is suggested to be due to the change in topography at Cape Hatteras and the fact that the GS separates from the coast there. In the SAB, the GS flows closer to the coast so the coastal response to changes in the GS is much larger than changes in the MAB, after the GS moved away from the coast. The disruption to the GS flow seems to generate southward propagating coastal waves, as seen also in other studies (Ezer, 2016). Another interesting result is the large variations in coastal sea level over short time scales in the SAB and the somewhat unexpected result that cold and warm anomalies are far from being a mirror image of each other. In the case of warm anomaly (Fig. 3a), coastal sea level dropped by as much
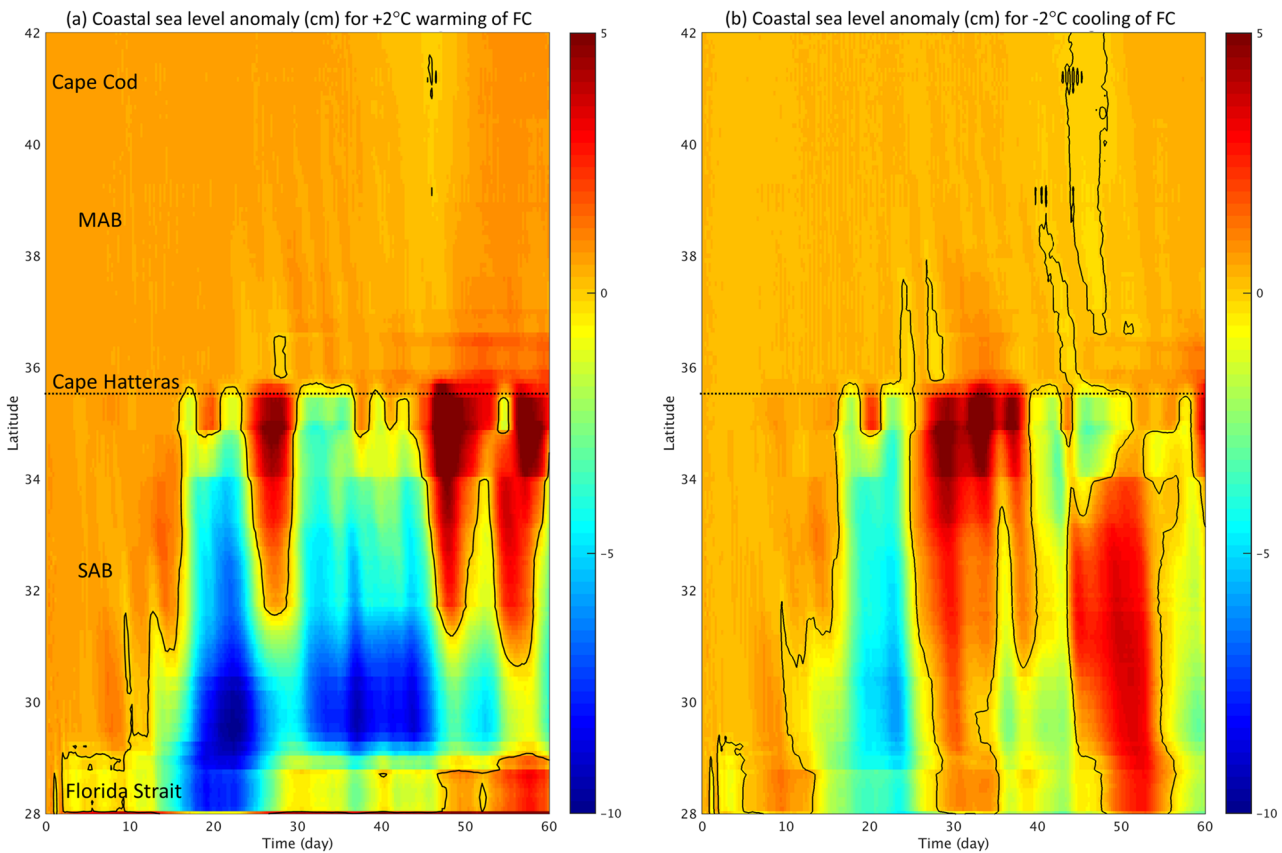

Fig. 3 Hovmöller plot of sea level anomaly (relative to the control case) along the coast (*y*-axis) versus time (*x*-axis) for **a** the FC warming experiment and **b** the cooling experiment. The black contour is zero with blue and red colors represent negative and positive coastal sea level, respectively. Horizontal dash line is the latitude around Cape Hatteras, separating between the Mid-Atlantic Bight (MAB) and the South Atlantic Bight (SAB), and where the Gulf Stream separates from the coast

as 10 cm, but after ∼ 50 days, sea level increased in the northern part of the SAB. The initial decrease in sea level along the coast suggests that the warm anomaly caused intensification of the FC (Ezer 2016), and this hypothesis will be tested later. Increased coastal sea level near Cape Hatteras after 50 days may indicate that warm anomalies advected downstream and reached the coast, and this also will be tested later. The response to cold anomalies (Fig. 3b) is about half (∼ 5 cm) of the response to warm anomalies with raising coastal sea level after 30 and 50 days, potentially inducing some long waves or meanders along the FC.

The time evolution of coastal sea levels at 3 locations (MAB, Cape Hatteras, and SAB) for experiments FC ± 2, SC ± 2, and SS ± 2 are shown in Figs. 4, 5, and 6, respectively. As mentioned before, the impact of FC anomalies on the MAB is quite small (less than ∼ 1 cm) (Fig. 4a) compared with variations over 10 cm in the SAB (Fig. 4c). The fact that warm and cold anomalies cause decrease and increase coastal sea level, respectively, is consistent with the change in the geostrophic flow of the FC (i.e., warmer GS has larger temperature difference relative to the colder coastal waters and larger sea level slope across the current). The changes

Fig. 4 Coastal sea level at **a** 37° N (MAB), **b** 35° N (near Cape Hatteras), and **c** 30°N (SAB), for the FC warming (red) and FC cooling (blue) experiments. Note the different scale of each panel
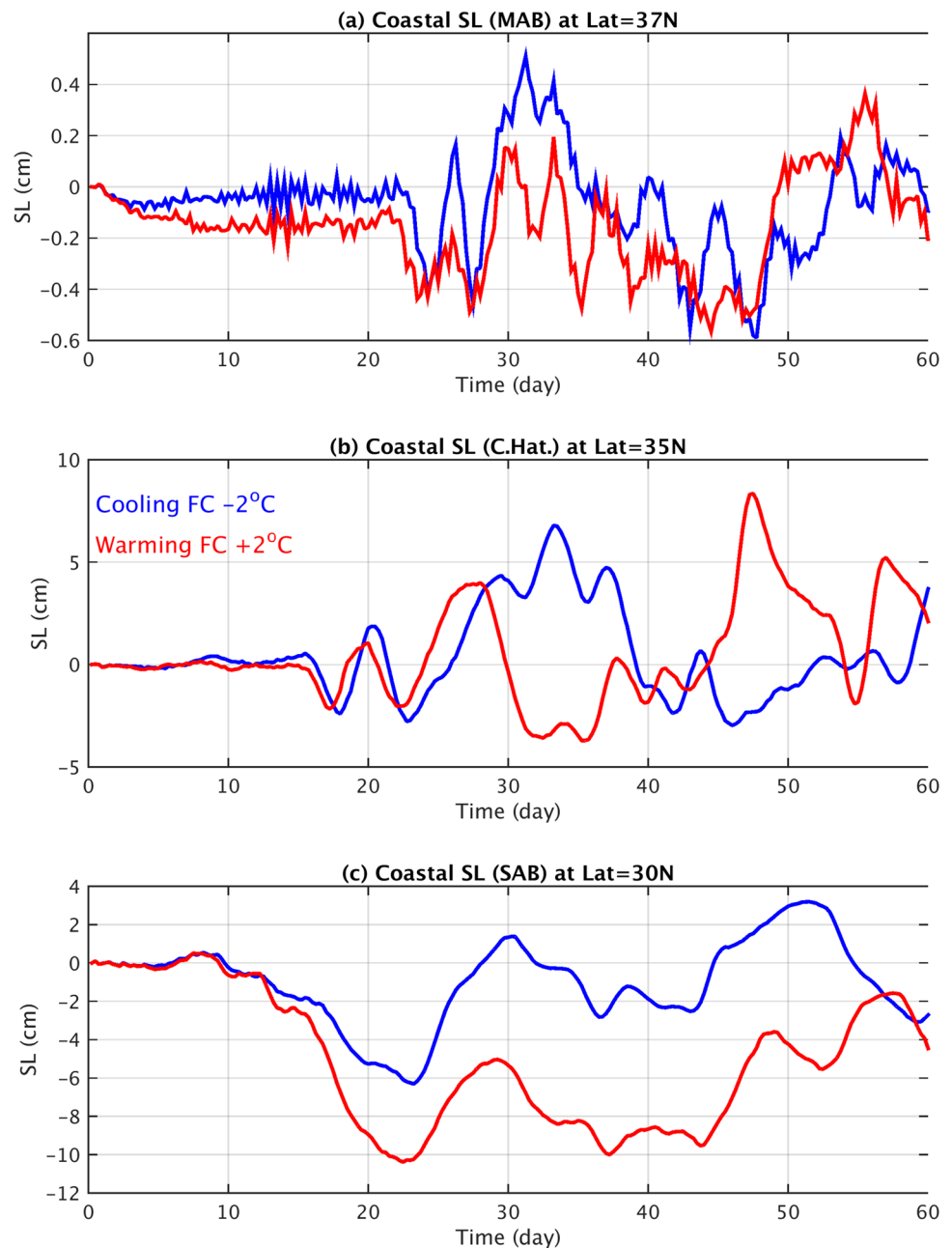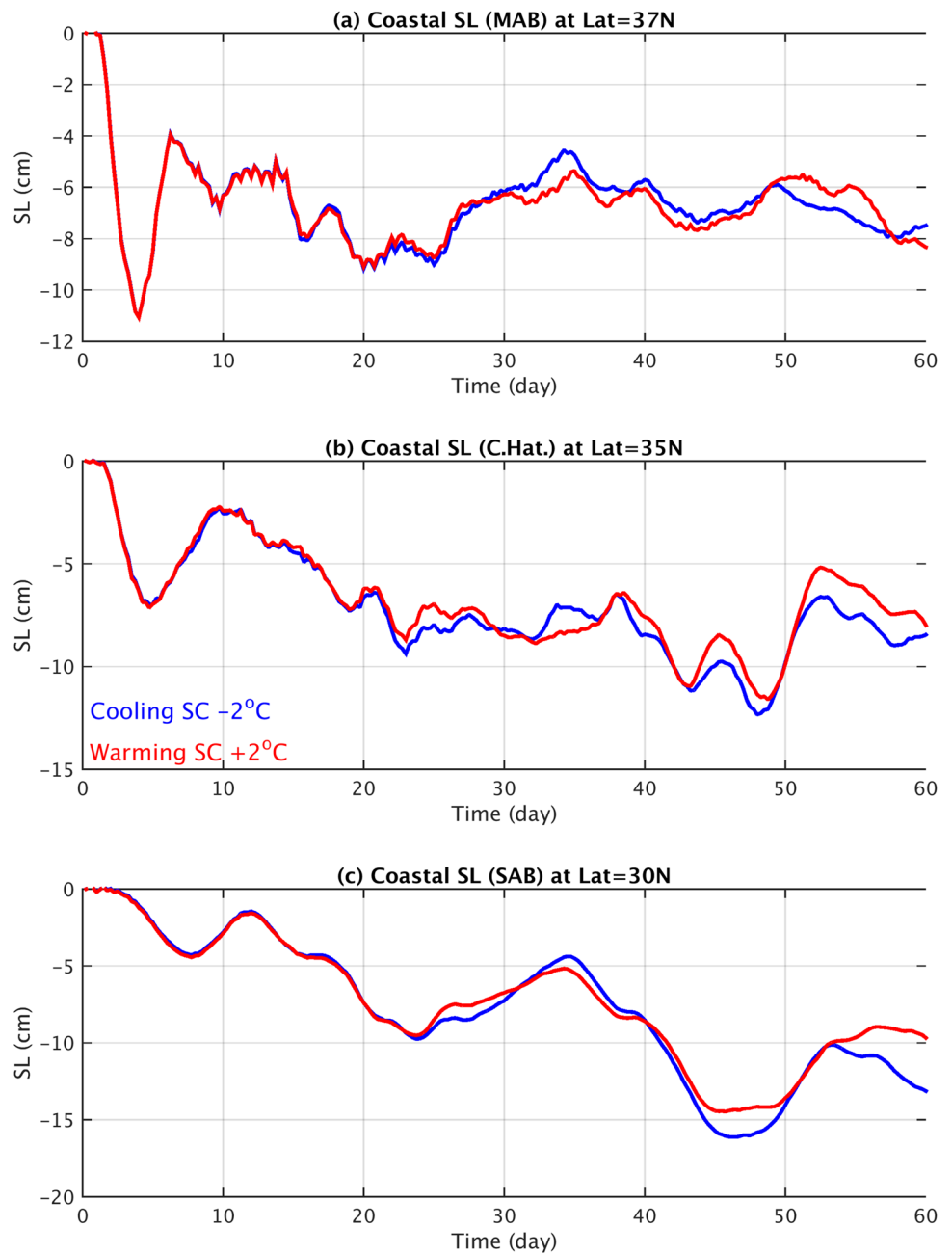
Fig. 5 Same as Fig. 4, but for SC warming and cooling cases

(a) Coastal SL (MAB) at Lat=37N

(b) Coastal SL (C.Hat.) at Lat=35N

Cooling SC −2°C
Warming SC +2°C

(c) Coastal SL (SAB) at Lat=30N

in sea level near Cape Hatteras on the other hand are interesting, whereas warming caused sea level to first drop by ~ 3 cm then to raise by ~ 8 cm, but cooling caused an opposite response, first raising sea level and then dropping sea level. However, the warming and cooling cases are not perfectly anticorrelated, which indicates strong nonlinearity in the system. The suggested mechanism is as follows: the initial response reflects changes in the GS flow (Ezer 2016 shows barotropic response to changes in FC flow within hours to few days), but then when the anomalies advected downstream by the currents and reach Cape Hatters

after ~ 30 days (Fig. 2), the thermosteric effect reverses the sea level trend. Note that near Cape Hatteras the GS is the closest to the coast, so anomalous GS waters may be felt near the coast. Unlike the FC ± 2 experiments that show large differences between cold and warm anomalies (Fig. 4), anomalies in the Slope Current in experiments SC ± 2 resulted in similar coastal sea level variations whether they are cold or warm (Fig. 5)— as will be seen later, disruption in the Slope Current seemed to affect the position of the GS more than its strength. Temperature anomalies in the Sargasso Sea in experiments SS ± 2 also show differences between

Fig. 6 Same as Fig. 4, but for SS warming and cooling cases
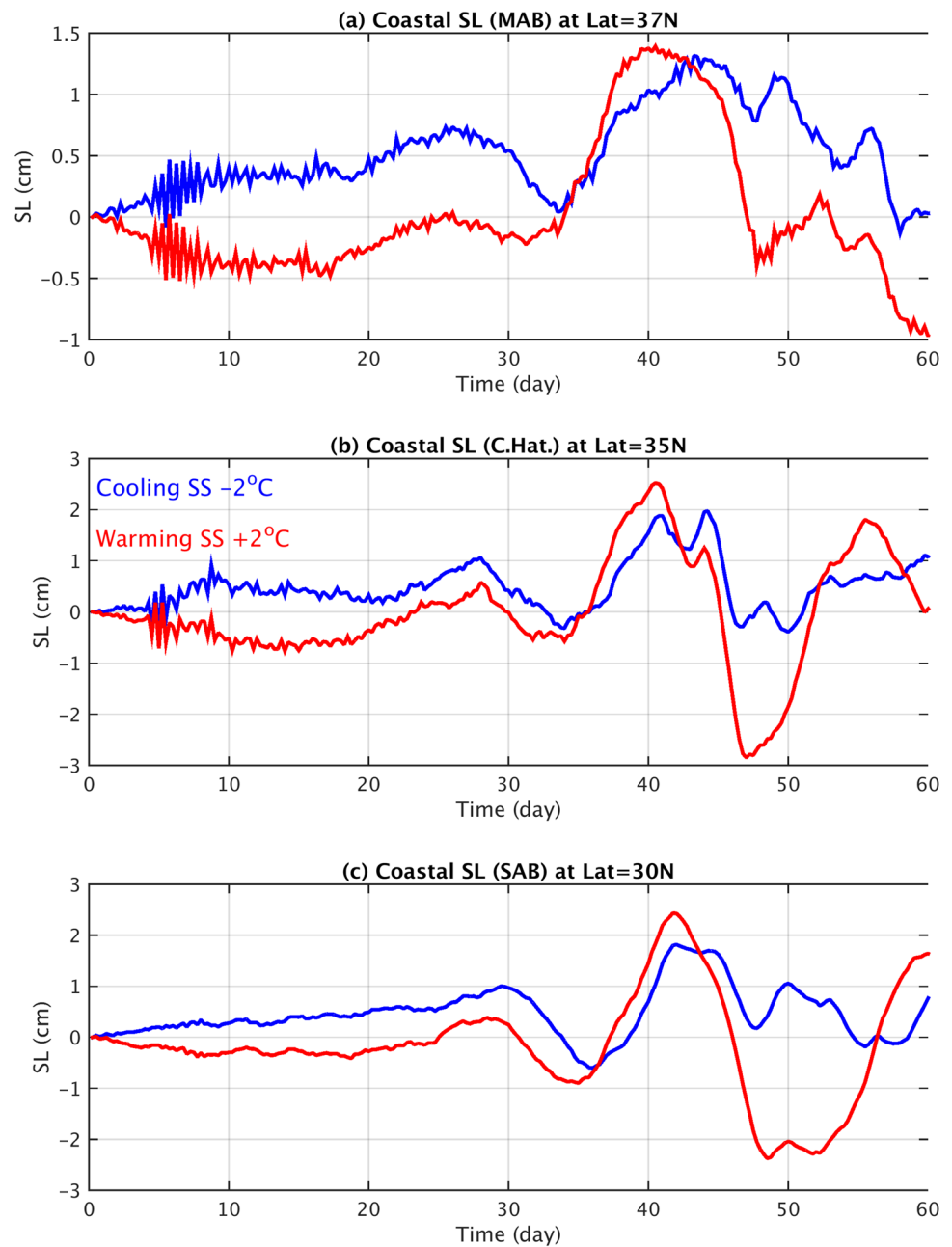
the coastal sea level response to cooling and warming (Fig. 6), but the total change (< 3 cm) is smaller by a factor of 2–3 that the changes induced by the FC (Fig. 4). Qualitatively, the relatively lower coastal sea level in the warming cases compared with the cooling cases supports again the suggestion that warming of the GS or the Sargasso Sea and the subtropical gyre will enhance the geostrophic flow of the GS by increasing gradients of temperature and thus increasing sea level gradients across the GS.

3.2 The impact of temperature anomalies on the Gulf Stream

Cross section of sea level and velocity across the GS in the MAB and the SAB are shown for all the experiments after 60 days in Figs. 7, 8, and 9. The most pronounced impact on the GS is the case of FC warming (red lines in Fig. 7) which increased the sea level difference across the GS by as much as ∼ 20 cm (Fig. 7a, b) and the maximum velocity by as much as 0.5–1.0 m/s (Fig. 7c, d) relative to the control case. The cooling FC case (blue lines in Fig. 7) had smaller impact than

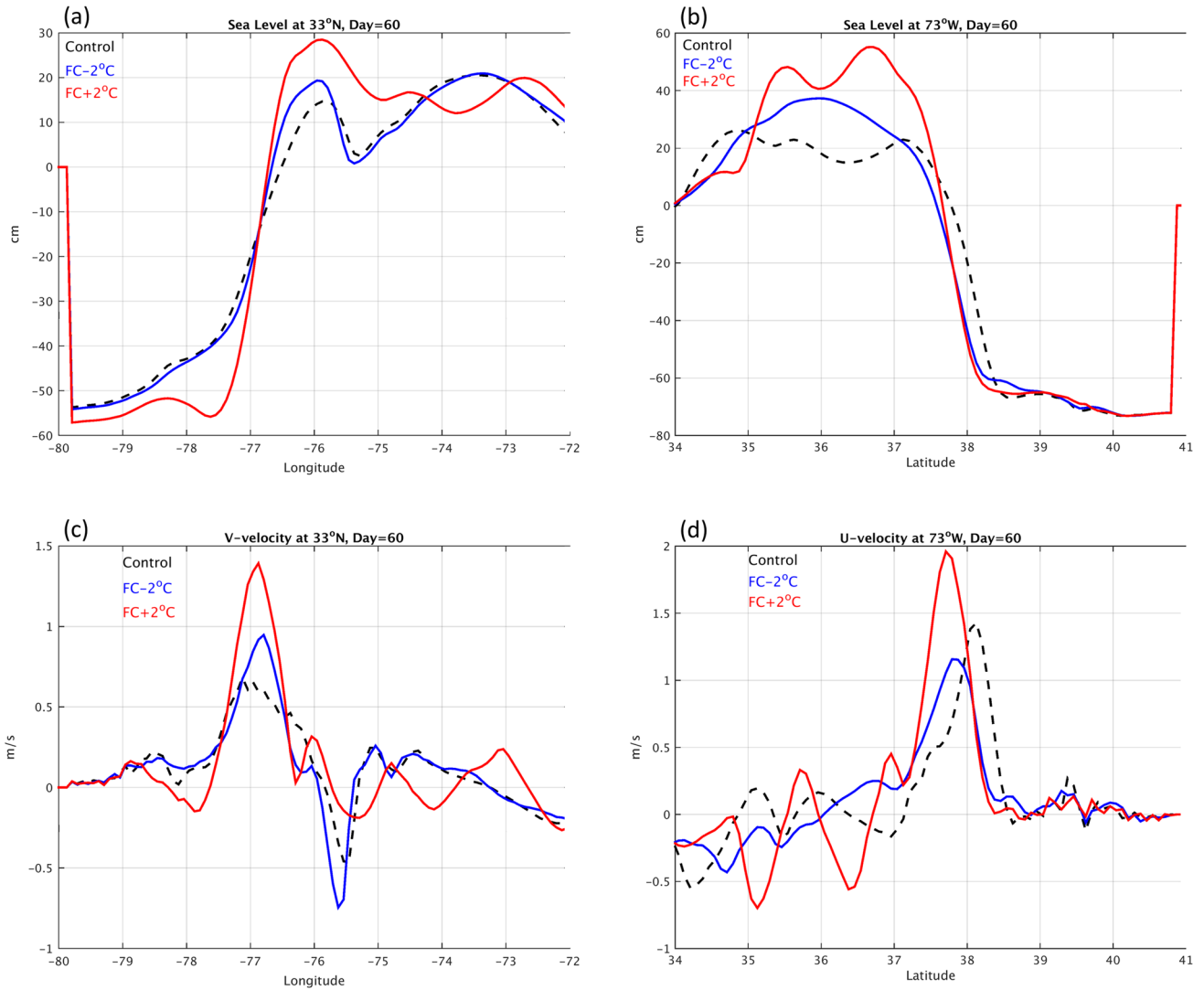## Temperature Anomaly in Florida Current (FC)

Fig. 7 Sea level (top panels) and velocity (bottom panels) along west–east cross section at 33° N (left panels; SAB) and along south to north cross section (right panels; MAB). Dash, red, and blue lines are for the control case, the FC warming case, and the FC cooling case, respectively. The coast is on the left/right side in the left/right panels

warming, but interestingly enough, both cases, FC + 2 and FC-2, caused similar offshore (southward) shift in the GS path (~ 30 km) in the MAB (Fig. 7b, d), but no shift is seen in the SAB (Fig. 7a, c) where the anomaly entered. This result is consistent with some previous studies that link variations in the GS strength to its path; for example, Ezer (2015) found significant negative correlation between the transport of the FC and the position of the downstream GS in the MAB, so that stronger GS would imply a southward shift, as seen here. Experiments with anomalies coming from the north (Fig. 8) show very little difference between warming (SC + 2) and cooling (SC-2) experiments, but in both cases, there was a significant impact on the

GS position with a shift of ~ 30 km offshore (eastward) in the SAB (Fig. 8a) and ~ 50 km inshore (northward) in the MAB (Fig. 8b). The maximum velocity of the GS increased in the SAB (Fig. 8c) but decreased in the MAB (Fig. 8d). The increase in the maximum GS velocity (~ 0.4 m/s; Fig. 8c) in the SAB is consistent with the drop (~ 10 cm; Fig. 8a) in coastal sea level, but this is not the case in the MAB where coastal sea level also dropped. It seems that the disruption to the SC and the recirculation gyre north of the GS, together with the large northward shift in the GS path in the MAB, are the causes for the sea level drop there. Temperature anomalies in the Sargasso Sea (Fig. 9) had relatively smaller influence on the GS flow and sea level and only
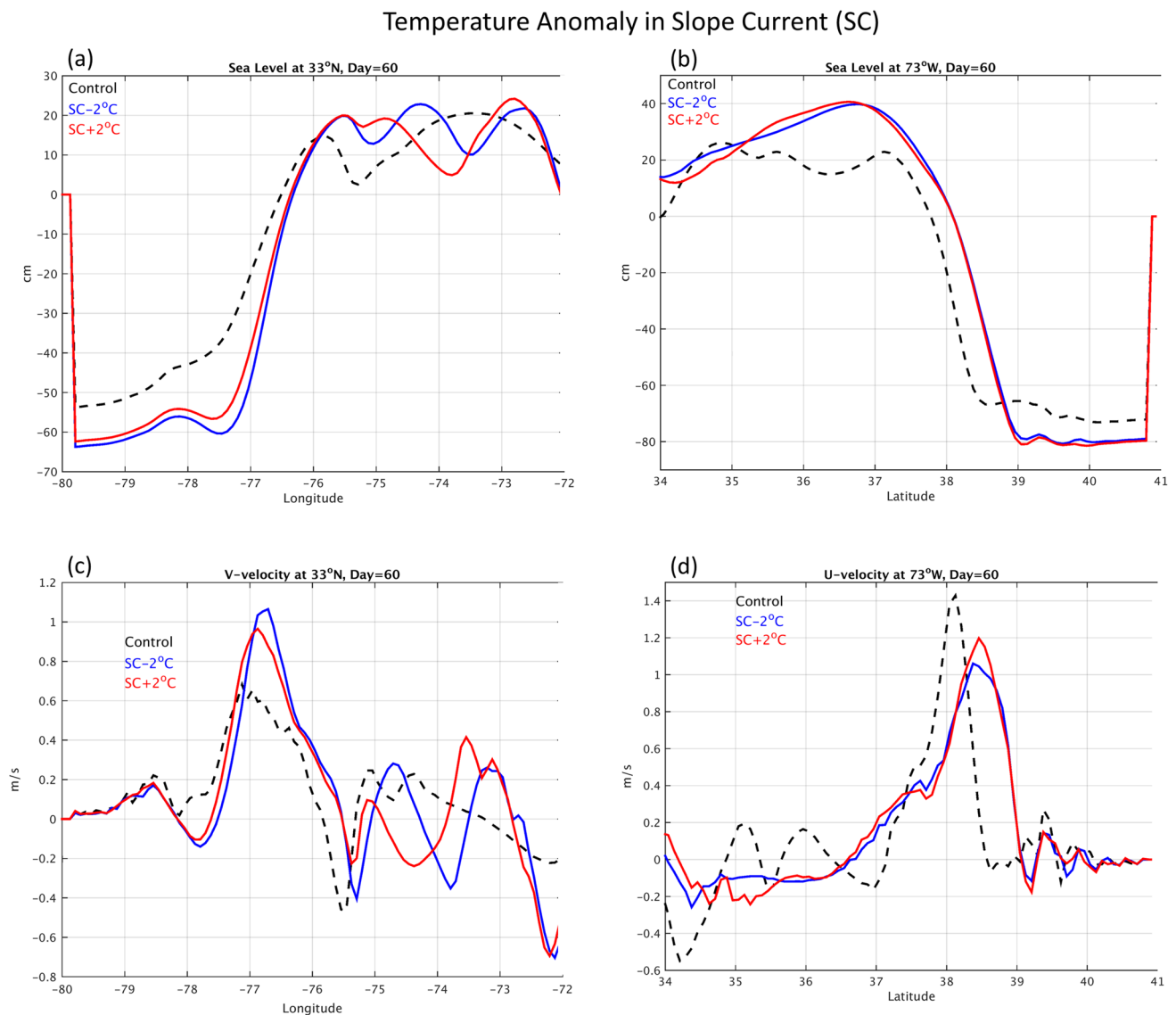
Temperature Anomaly in Slope Current (SC)

Fig. 8 The same as Fig. 7, but for warming and cooling of the SC

small differences between cooling and warming cases. Significant influence of the temperature anomalies on sea level and velocity are seen mostly as increased variability in the subtropical gyre away from the coast, east of 75° W off the SAB (Fig. 9a, c) and south off 36° N off the MAB (Fig. 9b, d). A very small offshore shift in the GS position is also seen when the SS is disrupted by temperature anomalies. Because of the non-linear and unpredictable nature of the response, it is not possible to predict the combined impact of anomalies that simultaneously appear at different locations, but such additional experiments seem interesting to conduct in the future.

3.3 Kinetic energy and relation of coastal sea level to temperature and currents

Studies suggest that western boundary currents (WBCs) are sensitive to global climate change, which can be detected when WBCs change their intensity, position, and eddy activities (Wu et al. 2012; Beal and Elipot 2016; Yang et al 2016). For example, based on sea level reconstruction since 1900, Ezer and Dangendorf (2021) showed that uneven warming near WBCs creates temperature and sea level anomalies that will enhance kinetic energy, while variations in the wind had lesser role. Therefore, it is useful to examine if introducing temperature anomalies in the model would have similar enhanced kinetic

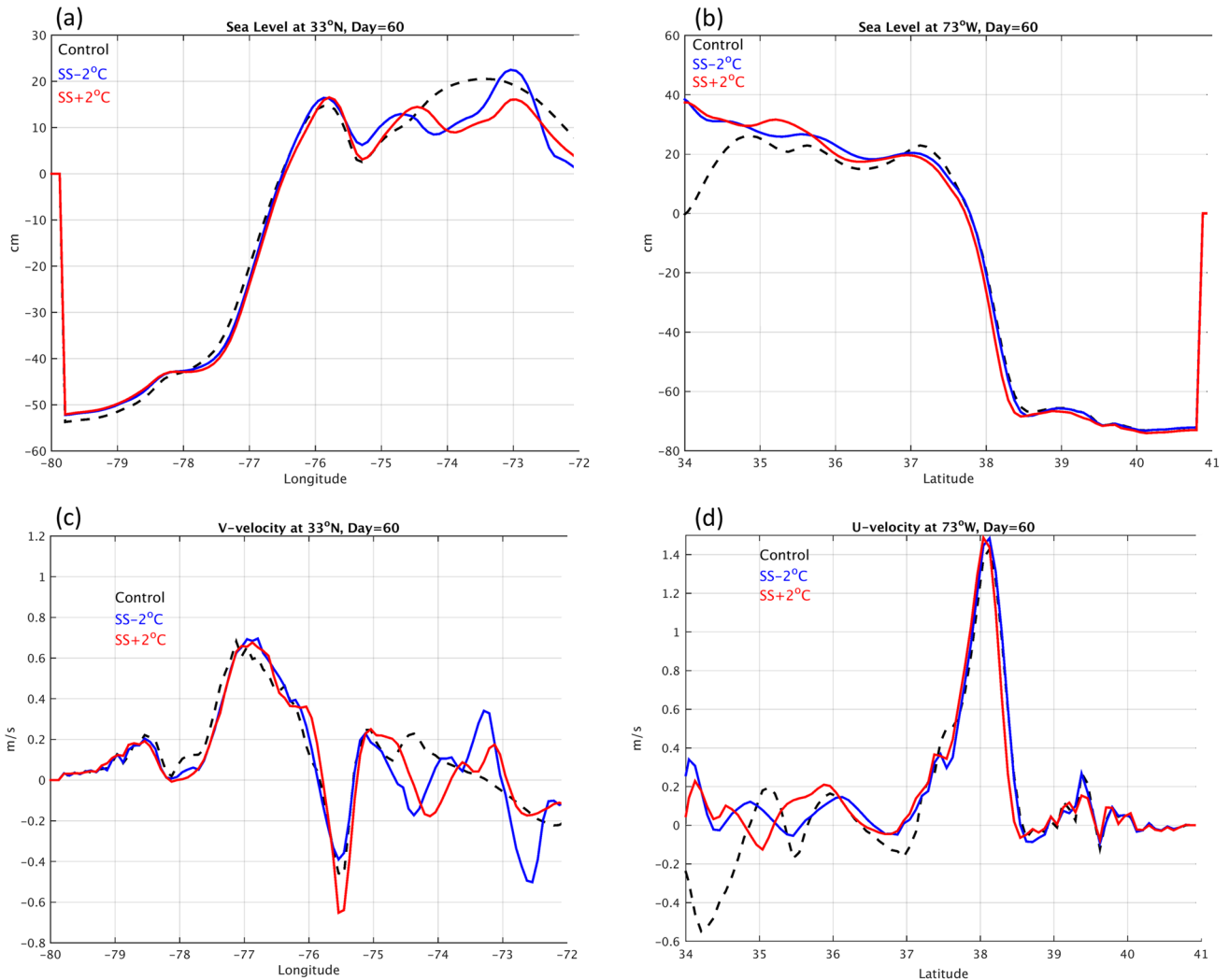## Temperature Anomaly in Sargasso Sea (SS)

Fig. 9 The same as Fig. 7, but for warming and cooling of the SS

energy as seen in observations. Figure 10 indeed indicates increased kinetic energy in all the cases with temperature anomalies. While in all cases temperature anomalies enhanced the area-mean surface kinetic energy over the model domain, the magnitude of the impact depends strongly on the location of the anomaly. The largest response is in the FC + 2 case (red line in Fig. 10a) where warm anomaly is injected directly into the GS and advected fast downstream by the current (Fig. 2). As indicated before, the GS velocity significantly increased in this case (Fig. 7). The FC ± 2 experiments are also the only cases where warming and cooling impacted kinetic energy very differently (Fig. 10a), while in the other experiments (Fig. 10b, c), the difference between warming and cooling was relatively small. The only case where cold anomaly increased kinetic energy more than warm anomaly was case

SC-2 (blue line in Fig. 10b); this may be explained by the fact that colder waters entering from the north could enhance the cold, southward flowing Slope Current and increase gradients relative to the warmer GS. The SS ± 2 cases had the smallest impact (Fig. 10c) since anomalies in the Sargasso Sea enter the domain in a region with less mesoscale activity and farther away from the GS, so that advection of anomalies is slower than in the other experiments.

4 Summary and conclusions

The study aimed at understanding the dynamic response of the GS system and the coast to impact of temperature anomalies; these anomalies can result from disruption
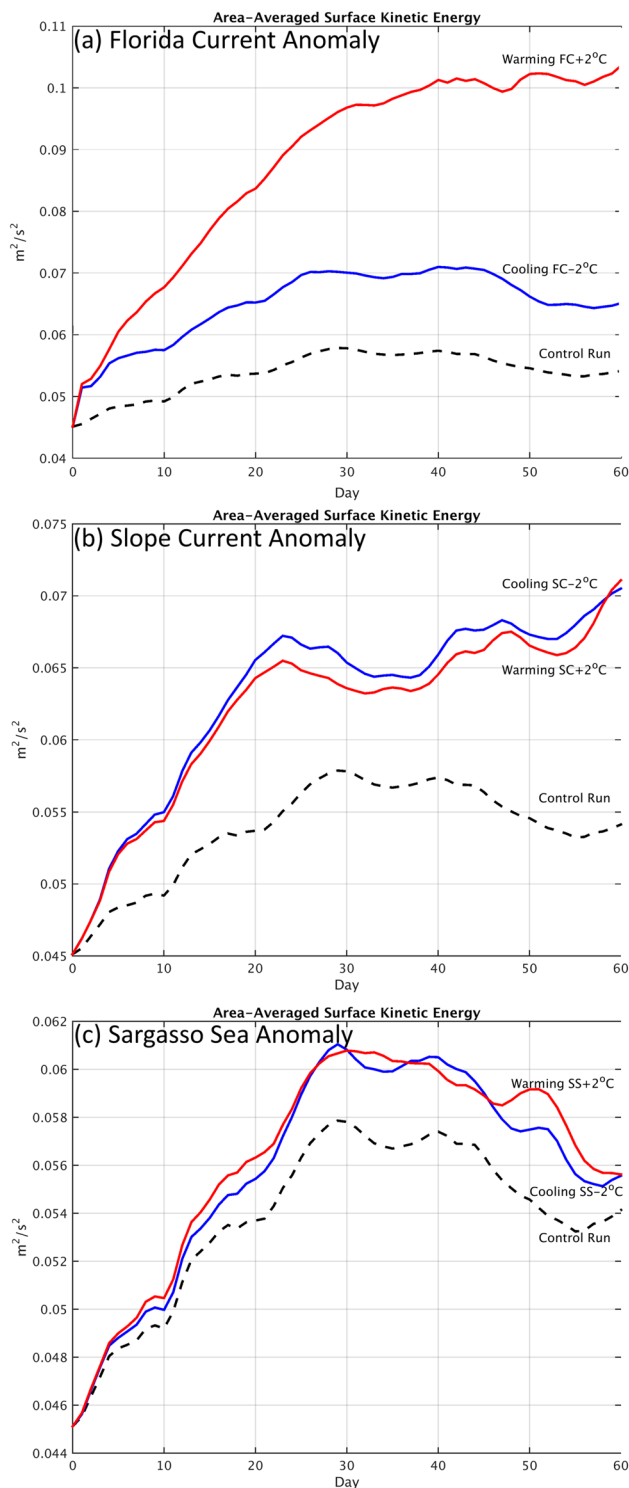
Fig. 10 Area averaged surface kinetic energy over the model domain for **a** FC warming (red)/cooling (blue), **b** SC warming/cooling, and **c** SS warming/cooling. The control case in dash line is the same for all cases but is plotted with different scales to highlight the differences

Fig. 11 A summary diagram of coastal sea level changes at 35° N (near Cape Hatteras) during 60-day simulations. Red and blue bars represent warming and cooling cases respectively for each of the 3 boundary conditions where temperature anomalies were imposed (FC, SC, and SS). Also shown are the correlations of coastal sea level at 35° N with near-coast surface temperature (R_{Tmp}) and the off-shore GS surface velocity (R_{GS}); only correlations with confidence level > 95% are listed

of the GS by hurricanes (Ezer et al. 2017; Ezer 2018, 2019b, 2020; Kourafalou et al. 2016; Todd et al. 2018), by other weather events, or by climatic changes in the
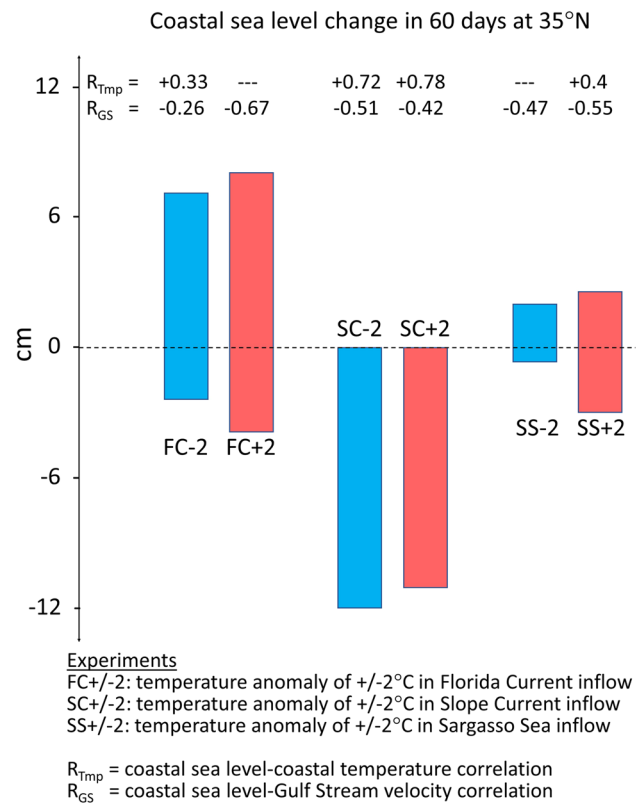
Atlantic Warm Pool (Domingues et al. 2018). Past studies indicated that anomalies entering western boundary current systems would have an impact on ocean currents and sea level within days due to the strong currents and meso-scale eddy activities. Since sea level along the US East Coast and the risk of coastal flooding are linked with variations in the GS (Ezer et al. 2013; Ezer and Atkinson 2014; Ezer, 2016; Wdowinski et al. 2016), a better understanding of potential remote influences on the coast has important implications for efforts involved coastal resilience and adaptation to climate change. The study conducted here, used idealized model experiments to examine the influence of the location of temperature anomaly on the dynamic response. Such sensitivity experiments may not try to closely imitate the real ocean, but rather to study processes under controlled conditions that are not possible in the real ocean. In each experiment, warm or cold anomaly entered the model domain from one of three possible inflow currents while holding the other boundary conditions unchanged and

neglecting any surface air-sea interaction (constant wind and nil heat flux). It should be noted that in the real ocean, after long enough period, air sea interaction would impact the surface anomalies through feedbacks and changes in surface wind and heat fluxes, but here, only the immediate short-term dynamic response is accounted for.

Figure 11 provides a summary of the impact on coastal sea level near Cape Hatteras from the 6 different anomaly experiments; for each case, correlation of coastal sea level with nearby temperature and with the GS flow offshore Cape Hatters are calculated, to assess the influence of these two factors. Qualitatively, it is shown that temperature anomaly of 2 °C can induce about 5–12 cm change in coastal sea level, about 0.5–1.0 ms^{-1} change in surface velocity, and about 30–50 km shift in the GS position. The experiments show that the response is not linearly related to the temperature anomaly, i.e., warm and cold anomalies do not result in opposite response but rather in a disruption of ocean currents and somewhat unpredictable sea level variations. Therefore, after 60 days warm and cold anomalies in the FC tend to increase sea level near Cape Hatteras, while the same anomalies in the SC tend to decrease sea level at Cape Hatteras. Because of the change in topography and the separation of the GS from the coast at Cape Hatteras, sea level north and south of that point often responds in opposite direction, as seen in several other studies (Ezer 2016, 2019a; Woodworth et al. 2016; Valle-Levinson et al. 2017; Domingues et al. 2018). Short-term variations in coastal sea level are driven here by two competing mechanisms, thermosteric sea level induced by the temperature anomalies and dynamic sea level induced by variations in the strength and position of the GS (i.e., due to the geostrophic balance, a stronger GS flow has grater sea level slope across the current with higher sea level offshore and lower sea level near the coast). In all cases, coastal sea level near Cape Hatteras is positively correlated with temperatures (maximum correlations of 0.78 in the SC + 2 experiment; Fig. 11) and negatively correlated with the GS flow (largest anticorrelation of − 0.67 in the FC + 2 experiment). This correlation pattern can create opposing impacts on the coast—increased temperature near the coast would raise sea level due to the thermosteric effect, but increased temperature offshore near the GS would lower coastal sea level due to increased gradients across the GS and the geostrophic balance. The combination of the two factors results in unusual sea level variability where, for example, in the FC + 2 experiment sea level, downstream initially

dropped due to strengthening of the GS, but later when warm anomalies propagated downstream, thermosteric effects start to dominate and increase coastal sea level. Anomalies introduced in the Sargasso Sea had somewhat smaller impact since they enter the domain in a region with weaker currents and less meso-scale activity.

While the sensitivity experiments with an idealized model configuration and controlled conditions are meant to study processes and not simulate the real ocean, it is constructive to see if the variability obtained by the model is at least qualitatively consistent with observed ocean variability. As an example, observations were obtained for a period of 3 months (August–November 2017), a period in which 3 hurricanes passed the study area (Fig. 12) and generating short-term variabilities like that in the model experiments. Observations showed that these 3 hurricanes, Irma, Jose, and Maria, disrupted the GS flow (Todd et al. 2018), which is another element simulated here. The observations used here include temperature and coastal sea level (from NOAA's Tide and Currents data set) in the northern and the southern parts of the SAB, and the observed Florida Current transport (from NOAA/AOML's cable data; Baringer and Larsen 2001; Meinen et al. 2010), they are shown in Fig. 13. During this 4-month period, temperature variations of ~ 2–5 °C and sea level variations of ~ 10–50 cm were observed with oscillations with periods of ~ 10–20 days. These amplitude and time scales are generally consistent with the model results (except storm surges that were not modeled). The three hurricanes that passed the region in September 10–28 (Fig. 12 and Fig. 13a) contributed to those variations. First, hurricane Irma passed over Florida's west coast, cooling the water by ~ 5 °C (Fig. 13a) and inducing a storm surge of ~ 1.2 m in Miami (blue line in Fig. 13b), but no storm surge in Cape Hatteras is seen since that hurricane moved west away from the coast after landfall in Florida (red track in Fig. 12). Then hurricanes Jose and Maria off the Atlantic coast (blue and green tracks in Fig. 12) induced storm surges of 0.6 and 0.8 m at Cape Hatteras (red lines in Fig. 13b). These consecutive hurricanes weakened the Florida Currents by ~ 10 Sv (Fig. 13c); this decline of the GS flow during these three 2017 hurricanes was observed by the FC cable and by gliders (Todd et al. 2018). During September when the FC transport weakened, coastal sea level rose, in agreement with this study and others that show anticorrelation between short-term variations in the GS and coastal sea level (e.g.,

Fig. 12 The tracks of three hurricanes that passed near the Gulf Stream in September 2017
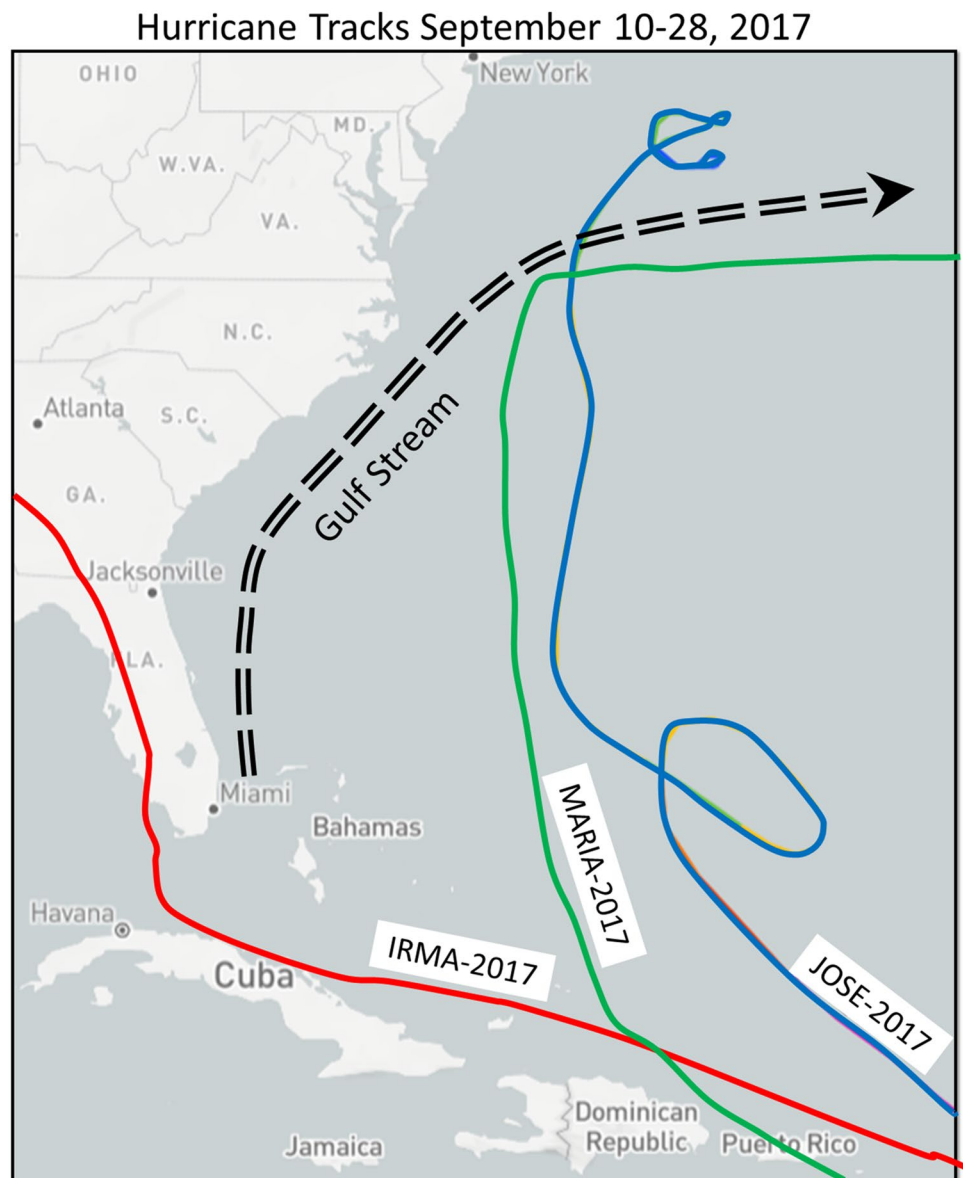

Ezer, 2016). When the FC reached its lowest transport in late September, sea level at Cape Hatteras reached its peak height, and when the FC reached a peak height in late October, a large drop in sea level is seen in Cape Hatteras. This immediate response of coastal sea level to changes in the GS flow is consistent with this model results and previous studies that show a fast barotropic response to changes in the FC transport. In contrast, baroclinic response due to temperature anomalies propagate at slower rate (Ezer 2018, 2020) and possible evidence for that is seen a month and a half after the hurricanes passed

when significant cooling is seen in Cape Hatteras in the middle of November (Fig. 13a). In the model, anomalies propagated from the Florida Strait to Cape hatters within about 20 days (Fig. 2 and Fig. 4b), with similar time scales seen in the observations.

Another interesting result from the sensitivity model experiments is that temperature anomalies near regions with strong currents and meso-scale variability can increase surface kinetic energy, especially if anomalies are injected into a current like the Gulf Stream (Fig. 10). This may have implications for the impact of climate change on ocean variability. Recent studies suggested, for example,

Fig. 13 Example of observations in the SAB during August-November 2017: **a** hourly water temperature, **b** hourly sea level anomaly, and **c** daily Florida Current transport. Temperature and sea level are from NOAA's tide gauge stations near Miami (at 25.7° N, in blue) and near Cape Hatteras (at 35.2° N, in red). The Florida Current transport is from NOAA/AOML cable measurements at 26.5° N. The period in September when 3 hurricanes passed the region is indicated in (**a**) (see Fig. 12 for hurricane tracks)
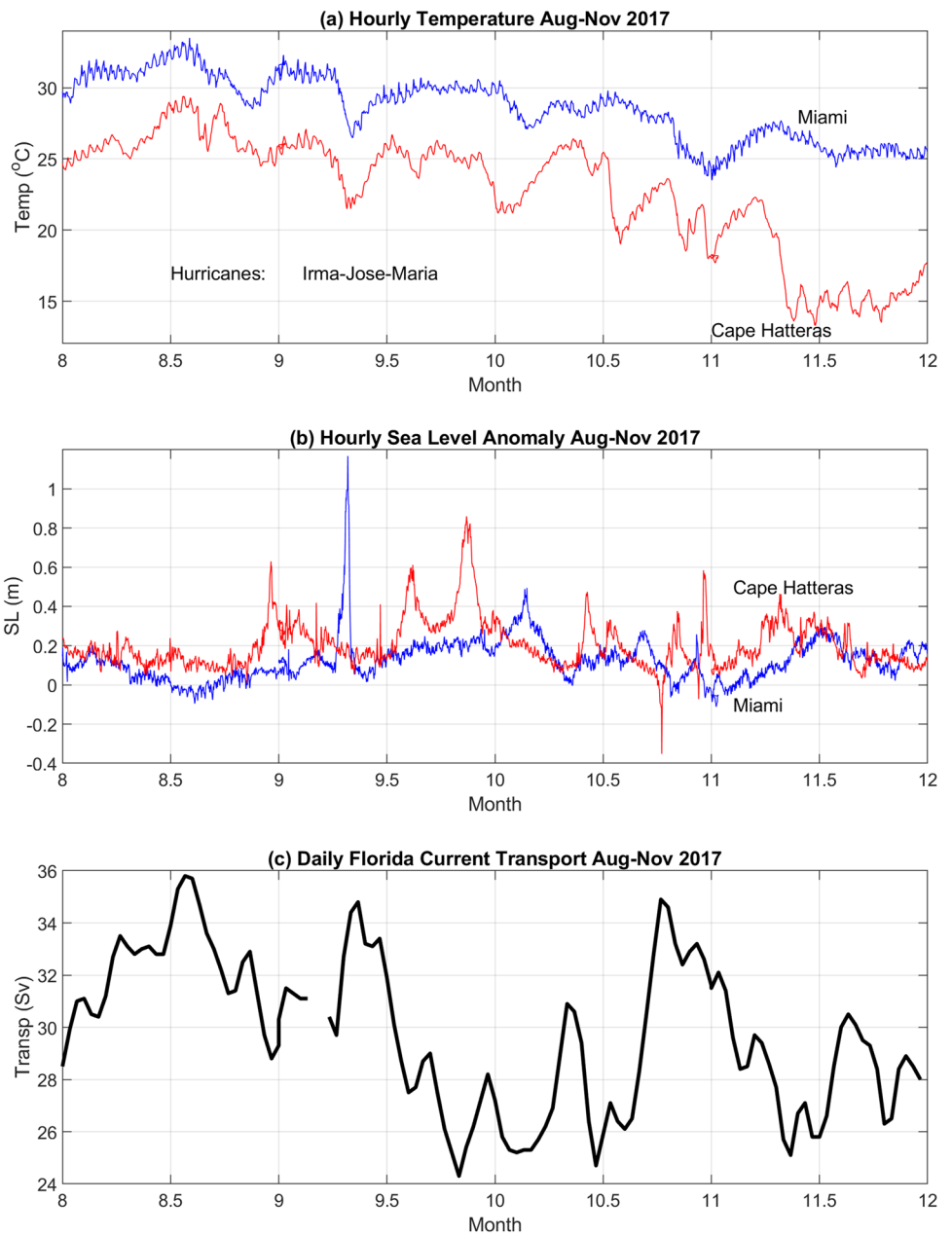
that observed upward trends in surface kinetic energy of western boundary currents are linked with uneven warming of these regions (Ezer and Dangendorf 2021). The model experiments demonstrated that the strength and the path of strong currents like the GS are very sensitive to the location of temperature anomalies, and this can result in unpredictable spatial and temporal variations in coastal sea level, with implications for sea level and flood prediction.

Declarations

Conflict of interest The authors have no conflict of interest.

References

Baringer MO, Larsen JC (2001) Sixteen years of Florida Current transport at 27ºN. Geophys Res Lett 28(16):3,179-3,182. https://doi.org/10.1029/2001GL013246

Beal LM, Elipot S (2016) Broadening not strengthening of the Agulhas Current since the early 1990s. Nature, 540.https://doi.org/10.1038/nature19853

Blaha JP (1984) Fluctuations of monthly sea level as related to the intensity of the Gulf Stream from Key West to Norfolk. J Geophys Res Oceans 89(C5):8033–8042. https://doi.org/10.1029/JC089iC05p08033

Calafat FM, Wahl T, Lindsten F, Williams J, Frajka-Williams E (2018) Coherent modulation of the sea-level annual cycle in the United States by Atlantic Rossby waves. Nat Commun 9:2571. https://doi.org/10.1038/s41467-018-04898-y

Dangendorf S, Frederikse T, Chafik L, Klinck J, Ezer T, Hamlington B (2021) Data-driven reconstruction reveals large-scale ocean circulation control on coastal sea level. Nat Clim Chang. https://doi.org/10.1038/s41558-021-01046-1

Diabaté ST, Swingedouw D, Hirschi JJM, Duchez A, Leadbitter PJ, Haigh ID, McCarthy GD (2021) Western boundary circulation and coastal sea-level variability in Northern Hemisphere oceans. Ocean Sci 17:1449–1471. https://doi.org/10.5194/os-17-1449-2021

Domingues R, Goni G, Baringer N, Volkov D (2018) What caused the accelerated sea level changes along the U.S. East Coast during 2010–2015? Geophys Res Lett 45:13,367-13,376. https://doi.org/10.1029/2018GL081183

Goddard PB, Yin J, Griffies SM, Zhang S (2015) An extreme event of sea-level rise along the Northeast coast of North America in 2009–2010. Nat Comm 6:6345. https://doi.org/10.1038/ncomms7346

Ezer T (2001) Can long-term variability in the Gulf Stream transport be inferred from sea level? Geophys Res Let 28(6):1031–1034. https://doi.org/10.1029/2000GL011640

Ezer T (2015) Detecting changes in the transport of the Gulf Stream and the Atlantic overturning circulation from coastal sea level data: the extreme decline in 2009–2010 and estimated variations for 1935–2012. Glob Planet Change 129:23–36. https://doi.org/10.1016/j.gloplacha.2015.03.002

Ezer T (2016) Can the Gulf Stream induce coherent short-term fluctuations in sea level along the U.S. East Coast?: A modeling study. Ocean Dyn 66(2):207–220. https://doi.org/10.1007/s10236-016-0928-0

Ezer T (2018) On the interaction between a hurricane, the Gulf Stream and coastal sea level. Ocean Dyn 68:1259–2127. https://doi.org/10.1007/s10236-018-1193-1

Ezer T (2019a) Regional differences in sea level rise between the Mid-Atlantic Bight and the South Atlantic Bight: is the Gulf Stream to blame? Earth's Future 7(7):771–783. https://doi.org/10.1029/2019EF001174

Ezer T (2019b) Numerical modeling of the impact of hurricanes on ocean dynamics: sensitivity of the Gulf Stream response to storm's track. Ocean Dyn 69(9):1053–1066. https://doi.org/10.1007/s10236-019-01289-9

Ezer T (2020) The long-term and far-reaching impact of hurricane Dorian (2019) on the Gulf Stream and the coast. J Mar Sys 208https://doi.org/10.1016/j.jmarsys.2020.103370

Ezer T, Atkinson LP (2014) Accelerated flooding along the U.S. East Coast: On the impact of sea-level rise, tides, storms, the Gulf Stream, and the North Atlantic Oscillations. Earth's Future 2(8):362–382. https://doi.org/10.1002/2014EF000252

Ezer T, Mellor GL (2004) A generalized coordinate ocean model and a comparison of the bottom boundary layer dynamics in terrain-following and in z-level grids. Ocean Mod 6(3–4):379–403. https://doi.org/10.1016/S1463-5003(03)00026-X

Ezer T, Atkinson LP, Corlett WB, Blanco JL (2013) Gulf Stream's induced sea level rise and variability along the U.S. mid-Atlantic coast. J Geophys Res Oceans 118:685–697. https://doi.org/10.1002/jgrc.20091

Ezer T, Atkinson LP, Tuleya R (2017) Observations and operational model simulations reveal the impact of Hurricane Matthew (2016) on the Gulf Stream and coastal sea level. Dyn Atmos Oceans 80:124–138. https://doi.org/10.1016/j.dynatmoce.2017.10.006

Ezer T, Dangendorf S (2021) Variability and upward trend in the kinetic energy of Western Boundary Currents over the last century: impacts from barystatic and dynamic sea level change. Clim Dyn 57(9–10):2351–2373. https://doi.org/10.1007/s00382-021-05808-7

Hong BG, Sturges W, Clarke AJ (2000) Sea level on the U.S. east coast: decadal variability caused by open ocean wind-curl forcing. J Phys Oceanogr 30:2088–2098. https://doi.org/10.1175/1520-0485(2000)030%3c2088:SLOTUS%3e2.0.CO;2

Kohyama T, Yamagami Y, Miura H, Kido S, Tatebe H, Watanabe M (2021) The Gulf Stream and Kuroshio Current are synchronize. Science 374:341–346. https://doi.org/10.1126/science.abh3295

Kourafalou VH, Androulidakis YS, Halliwell GR, Kang HS, Mehari MM, Le Hénaff M, Atlas R, Lumpkin R (2016) North Atlantic Ocean OSSE system development: Nature Run evaluation and application to hurricane interaction with the Gulf Stream. Prog Oceanogr 148:1–25. https://doi.org/10.1016/j.pocean.2016.09.001

Little CM, Hu A, Hughes CW, McCarthy GD, Piecuch CG, Ponte RM, Thomas MD (2019) The relationship between U.S. east coast sea level and the Atlantic meridional overturning circulation: a review. J Geophys Res 124:6435–6458. https://doi.org/10.1029/2019JC015152

Meinen CS, Baringer MO, Garcia RF (2010) Florida Current transport variability: An analysis of annual and longer-period signals. Deep Sea Res 57(7):835–846. https://doi.org/10.1016/j.dsr.2010.04.001

Mellor GL, Hakkinen S, Ezer T, Patchen R (2002) A generalization of a sigma coordinate ocean model and an intercomparison of model vertical grids, In: Ocean Forecasting: Conceptual Basis and Applications, N. Pinardi and J. D. Woods (Eds.), Springer, 55–72. https://doi.org/10.1007/978-3-662-22648-3_4

Oey LY, Ezer T, Wang DP, Yin XQ, Fan SJ (2007) Hurricane-induced motions and interaction with ocean currents. Cont Shelf Res 27:1249–1263. https://doi.org/10.1016/j.csr.2007.01.008

Park J, Sweet W (2015) Accelerated sea level rise and Florida current transport. Ocean Sci 11:607–615. https://doi.org/10.5194/os-11-607-2015

Piecuch CG, Dangendorf S, Ponte R, Marcos M (2016) Annual sea level changes on the North American Northeast Coast: influence of local winds and barotropic motions. J Clim 29:4801–4816. https://doi.org/10.1175/JCLI-D-16-0048.1

Sallenger AH, Doran KS, Howd P (2012) Hotspot of accelerated sea-level rise on the Atlantic coast of North America. Nat Clim Change 2:884–888. https://doi.org/10.1038/NCILMATE1597

Todd RE, Asher TG, Heiderich J, Bane JM, Luettich RA (2018) Transient response of the Gulf stream to multiple hurricanes in 2017. Geophys Res Lett, 45https://doi.org/10.1029/2018GL079180

Valle-Levinson A, Dutton A, Martin JB (2017) Spatial and temporal variability of sea level rise hot spots over the eastern United States. Geophys Res Lett 44:7876–7882. https://doi.org/10.1002/2017GL073926

Wdowinski S, Bray R, Kirtman BP, Wu Z (2016) Increasing flooding hazard in coastal communities due to rising sea level: case study of Miami Beach, Florida. Ocean Coast Man 126:1–8. https://doi.org/10.1016/j.ocecoaman.2016.03.002

Woodworth PL, Maqueda MM, Gehrels WR, Roussenov VM, Williams RG, Hughes CW (2016) Variations in the difference between mean sea level measured either side of Cape Hatteras and their relation to the North Atlantic Oscillation. Clim Dyn 49(7–8):2451–2469. https://doi.org/10.1007/s00382-016-3464-1

Woodworth PL, Maqueda MAM, Roussenov VM, Williams RG, Hughes CW (2014) Mean sea-level variability along the northeast American Atlantic coast and the roles of the wind and the overturning circulation. J Geophys Res Oceans 119:8916–8935. https://doi.org/10.1002/2014JC010520

Wu L, Cai W, Zhang L, Nakamura H, Timmermann A, Joyce T, McPhaden MJ, Alexander M, Qiu B, Visbeck M, Chang P, Giese B (2012) Enhanced warming over the global subtropical western boundary currents. Nat Clim Chan 2:161–166. https://doi.org/10.1038/nclimate1353

Yang H, Lohmann G, Wei W, Dima M, Ionita M, Liu J (2016) Intensification and poleward shift of subtropical western boundary currents in a warming climate. J Geophys Res 121:4928–4945. https://doi.org/10.1002/2015JC011513